Energy Proceedings
Vol 51, 2025
ISSN 2004-2965

Modeling of high-temperature PEM fuel cell incorporating the combined effects of assembly pressure and gas diffusion layer thickness#

Hongxiang Zheng, Junwen Deng, Chuandong Li, Shuaishuai Yuan, Xinqi Yao, Feng Huang, Ruhang Zhang, Xinhai Yu*, Shan-Tung Tu

Key Laboratory of Pressure Systems and Safety (MOE), School of Mechanical and Power Engineering, East China University of Science and Technology, Shanghai, 200237, China

(*Corresponding Author. yxhh@ecust.edu.cn)

ABSTRACT

In this paper, a sequential model combining two-dimensional mechanical deformation and three-dimensional non-isothermal deformation was developed to investigate the combined effects of assembly pressure and gas diffusion layer (GDL) thickness on the structure and performance of a high-temperature proton exchange membrane fuel cell (HT-PEMFC). Through the utilization of the response surface methodology (RSM), it was determined that the HT-PEMFC exhibited its optimal overall performance when the assembly pressure was set at 1.38 MPa and the GDL thickness was 0.375 mm. Additionally, the study also delved into the effects of assembly pressure and GDL thickness on various aspects of the HT-PEMFC, including polarization curves, hydrogen distribution, oxygen distribution, and temperature distribution. It was observed that the temperature in the gas channel was consistently higher than in other solid regions.

Keywords: High temperature proton exchange membrane fuel cell; Assembly pressure; Gas diffusion layer thickness; Response surface methodology; Combined optimization.

1. INTRODUCTION

Over the past few years, high temperature proton exchange membrane fuel cell (HT-PEMFC) has garnered increasing attention due to several key advantages over low temperature proton exchange membrane fuel cell (LT-PEMFC) [1]. With operating temperatures ranging from 120-250°C, HT-PEMFC exhibits improved reaction kinetics at the electrodes, greater tolerance to impurities in fuel and air, simpler plate design, and better heat and water management [2].

In the process of assembling HT-PEMFC, a specific assembly pressure is typically applied to compress the fuel cell, thereby reducing the risk of gas leakage. Diedrichs et al. [3] conducted HT-PEMFC membrane electrode assemblies (MEA) compression experiments which revealed that the gas diffusion layer (GDL) thickness loss is the main source of MEA thickness loss. Therefore, the GDL is most susceptible to deformation due to its relatively low mechanical properties. Additionally, due to the structure of the bipolar plate (BP), some GDLs might intrude into the gas channels after compression, leading to changes in the thickness, porosity, and permeability of the GDLs. In contrast to LT-PEMFC, HT-PEMFC should also take into account the thermal expansion of the material at high temperatures and ignore the effects caused by humidity changes when studying the deformation of GDL. At the same time, water molecules exist as a gas at the operating temperature, and the mass transfer, temperature distribution, and electrochemical behavior of the HT-PEMFC could produce significant differences.

Diedrichs et al. [4] investigated the effect of compression force on the performance of high temperature polymer membrane fuel cells. It was found that when contact pressure (2 ~25 bar) was increased, the performance of MEA decreased consistently at low current densities, while the performance increased at higher current densities. On this basis, Pinar et al. [5] conducted contact pressure cycling tests in the range of 0.2-1.5 MPa, and the results showed that the compression force has an important effect on the performance of the HT-PEMFC, but causes damage to the whole MEA after exceeding a certain contact pressure. It was essential to choose an appropriate pressure range when assembling the fuel cell.

Tawfiq et al. [6] reported that a lower thickness of GDL within the range of 300~420 μm improved the performance of HT-PEMFC. However, the range of reported GDL thicknesses was relatively small, with HT-PEMFC GDL thicknesses ranging from 100 μm to 490 μm

This is a paper for the 16th International Conference on Applied Energy (ICAE2024), Sep. 1-5, 2024, Niigata, Japan.

in the literature [7, 8]. It was important to note that different conclusions may be drawn for other thickness ranges. In a study by Xia et al. [9], the effect of GDL thickness and porosity on flow uniformity, diffusive fluxes, and ohmic resistances of HT-PEMFC was investigated through parametric analysis. The results demonstrated that by controlling the thickness and porosity of the GDL, the performance of HT-PEMFC can be improved by 7.7%. While this article explored the effect of GDL thickness within a wide range, it did not take into consideration the impact of assembly pressure on the initiation of HT-PEMFC under real-world conditions.

Assembly pressure has multiple effects on the performance of HT-PEMFC. It alters the geometrical and physical properties of the GDL in the rib and airway sections, affecting the contact resistance of the fuel cell, and ultimately the local mass, heat, and charge transfer characteristics, which in turn affect the overall performance [10]. In addition, the thickness of the GDL plays an important role in these dynamics [11]. Thicker GDLs typically have better mechanical properties and are less prone to deformation under high assembly pressures, but also lead to an increase in overall ohmic resistance. In addition, different GDL thicknesses also affect the gas distribution within the fuel cell. Therefore, it is necessary to consider assembly pressure and GDL thickness as two important parameters at the same time and conduct a comprehensive study. Response surface methodology (RSM) is an effective mathematical and statistical method that has been widely applied to the study of proton exchange membrane fuel cells in recent years [12]. Therefore, the combined effects of assembly pressure and GDL thickness will be investigated using the RSM, allowing a more complete understanding of their impact on HT-PEMFC performance.

In this paper, the deformation of GDL under assembly pressures was investigated by a sequential study method using a two-dimensional half-cell model, and a three-dimensional HT-PEMFC model was reconstructed based on the deformation data. After model validation, the combined effects of both assembly pressure and GDL thickness were optimized using RSM. The results showed that the overall performance of HT-PEMFC was enhanced by about 9.24% at an assembly pressure of 1.38 MPa and a GDL of 375 μm. Finally, the effects of GDL deformation on HT-PEMFC hydrogen distribution, oxygen distribution, and temperature distribution were investigated.

2. MODEL DEVELOPMENT

2.1 Multiphysics model of HT-PEMFC

As shown in Fig. 1, the following sub-regions are considered in the HT-PEMFC modeling, including the BP, gas flow channels (CH), GDL, catalyst layer (CL), and phosphoric acid doped polybenzimidazole membrane (MEM). A finite element-based structural model was developed to simulate HT-PEMFC deformation for different assembly pressures and temperatures. After obtaining the deformation characteristics and material properties of the model, a Multiphysics field coupled fuel cell performance model was developed to analyze multi-component gas transport, chemical reactions, and charge transfer.

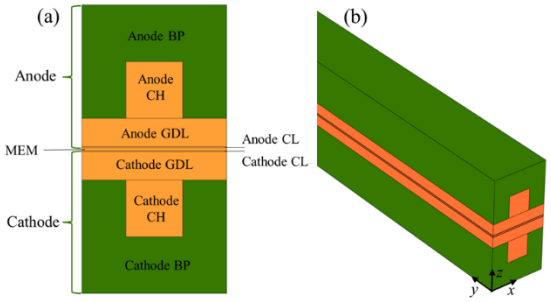

Fig. 1. Schematic diagram of the structure of HT-PEMFC (a). The 3D computational domain (b).

The operating temperature and pressure were 453.15 K and 1 atm, respectively. Both hydrogen and air humidification temperatures were 28 ℃. There were the following assumptions in this model:

(1) The fuel cell operated under steady-state conditions.
(2) The gas mixture was an ideal gas.
(3) The GDLs, CLs, and MEM were homogeneous, isotropic, and linear elastic materials.
(4) No liquid water formation during operation and laminar flow in the gas channel.

The anode gas mixture had hydrogen and water vapor, and the cathode gas mixture had oxygen, nitrogen, and water vapor.

Based on the assumptions made in the previous section, the governing equations of solid mechanics, mass, momentum, species, energy, and charge were applied to describe the complex physical processes of the fuel cell.

2.2 Boundary conditions

For the solid mechanics simulations, a 2D half-cell model is applied to study the stress-strain relationship of the fuel cell, while the temperature-induced thermal expansion is also considered, as shown in Fig. 2. Uniform

assembly pressure was applied to the top surface of the BP. The left and right boundary surfaces of the fuel cell were symmetric conditions. Therefore, the displacement was generated only in the z-direction, while no displacement was generated in the x-direction. In addition, a fixed constraint was set at the lower boundary of the membrane. The fuel cell clamping process only caused deformation in the GDL due to its lower Young's modulus compared to BP, MEM, and CL [13]. Furthermore, the interfacial resistance between BP and GDL in the computational domain of the fuel cell varied proportionally with changes in assembly pressure. In numerical calculations, simulating the change in interfacial resistance can be achieved through adjustments to the conductivity of the thin electrode layer.

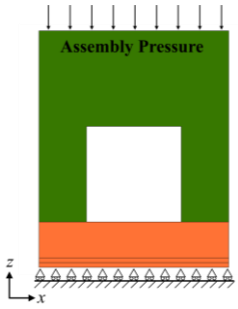

Fig. 2. Computational domain for solid mechanics analysis.

2.3 Numerical implementation

This study utilized the Multiphysics software COMSOL 6.0 to solve the stress-strain relationship of a fuel cell under two-dimensional conditions using the solid mechanics module. The resulting geometric deformation and physical characteristics, such as porosity and permeability, of the GDL deformed assembly were obtained. Subsequently, a three-dimensional non-isothermal model of high temperature proton exchange membrane fuel cell was constructed based on the deformation characteristics of the GDL. This model was used to investigate the steady-state transport phenomena in the flow channel, GDL, and CL, as well as the electrochemical kinetics in the GDL, CL, and proton exchange membrane. Additionally, the temperature distribution resulting from the electrochemical reactions was also studied.

3. RESPONSE SURFACE METHODOLOGY

In this study, RSM is applied to analyze the effect of assembly pressure and GDL thickness on the current density of the fuel cell using Mintab 21 (trial version) software based on the central composite design (CCD) methodology. The CCD employs two variables (assembly pressure and GDL thickness) to explore the effects on the current density. Table 1 lists the CCD test conditions for analyzing assembly pressure and GDL thickness. Considering the relationship between HT-PEMFC current density and voltage, Table 1 calculates the current density of the fuel cell at a voltage of 0.4V.

4. RESULTS AND DISCUSSIONS

4.1 Model validation

The numerical calculation results were compared to the experimental data of Yuan et al. [14] for model validation. The pressure, inlet gas composition, and operating temperature in the numerical model were generally consistent with the experimental conditions as reported in Ref [14], and the results are presented in Fig. 3. The anode and cathode stoichiometry ratios were set at 1.2 and 2.5, respectively. The fuel cell operated at 180°C, utilizing humidified hydrogen and air at atmospheric pressure.

In the high current density region, the simulation results agreed well with the experimental values, suggesting that the ohmic polarization loss was accurately simulated. However, in the low current density region, the simulation results were slightly higher than the experimental results. Overall, the predicted fuel cell current densities were in general agreement with the experimental data. Furthermore, based on the successful model validation, additional simulation calculations were conducted.

4.2 Optimization of assembly pressure and GDL thickness

From the literature [4, 7, 8], the assembly pressure of HT-PEMFC ranged from 0-2.5 MPa, and the thickness of GDL ranged from 0.1-0.5 mm. The computational design of the two factors of assembly pressure and GDL thickness is carried out by using the CCD method, as shown in Table 1. As shown in Fig. 4, both parameters have some effect on the current density. It could be calculated that the current density would reach a maximum value when the assembly pressure is 1.3878MPa and the GDL thickness is 0.3769mm. In the actual calculation, the parameters (assembly pressure = 1.38 MPa and GDL thickness = 0.375 mm) were selected to obtain a current density of 1.0129 A/cm^2 This value was within our 95% prediction interval (0.98952, 1.01495), which proved that this data was credible.

Utilizing the outcomes computed by the solid mechanics module, we reconstructed the HT-PEMFC model at operating temperature, which deforms at a

specific assembly pressure, and the results are presented in Fig. 5a. In the computation of the reconstructed 3D model, two supplementary factors necessitated consideration. Firstly, the porosity and permeability of the deformed GDL must be determined by Equations as previously stated. Secondly, the interfacial resistance between the GDL and BP was also subject to variation with changes in assembly pressure.

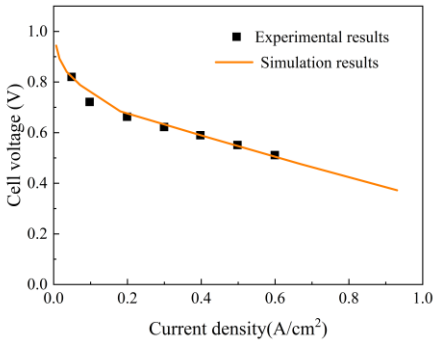

Fig. 3. Simulation results in comparison with experimental data.

Table 1. Calculation conditions for assembly pressure and GDL thickness.

Run	Assembly pressure (MPa)	GDL thickness (mm)	Current density (A/cm^2)
1	1.25	0.3	1.0012
2	1.25	0.3	1.0012
3	0	0.1	0.93556
4	1.25	0.3	1.0012
5	2.5	0.3	0.94873
6	0	0.3	0.93642
7	0	0.5	0.92063
8	1.25	0.3	1.0012
9	1.25	0.5	0.98761
10	1.25	0.1	0.98952
11	2.5	0.5	0.96684
12	1.25	0.3	1.0012
13	2.5	0.1	0.91158

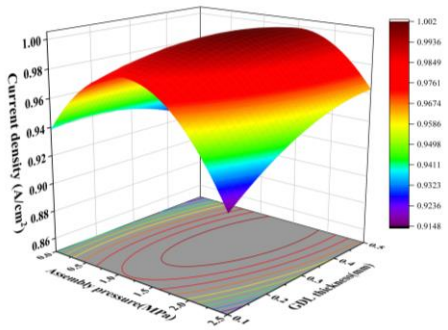

Fig. 4. Effect of assembly pressure and GDL thickness on HT-PEMFC current density.

Fig. 5b illustrates the polarization curves and power density curves of the optimized model given the cathode stoichiometry ratios of 2.5, 3.5, 4, and 5, respectively. Given the cathode stoichiometry ratios of 2.5, the current density increased from near 0 to 1.0129 A/cm^2 with the voltage of HT-PEMFC reduced from 0.95 to 0.4 V, while the power density rose from near 0 to 0.40516 W/cm^2. Similarly, for cathode stoichiometric ratios equal to 3.5, 4, and 5, the current density increased to 1.052, 1.0694, and 1.0794 A/cm^2, and the power density rose to 0.4208, 0.42776, and 0.43176 W/cm^2, respectively, with fuel cell voltages of 0.4 V. As the cathode stoichiometry ratio rose, the current density and power density of the HT-PEMFC started to increase and then stabilized. This was attributed to the increase in the cathode stoichiometry ratio led to a higher oxygen concentration, which consumed the hydrogen that was not involved in the reaction at the anode, eventually reaching a maximum limit [13].

To quantify the performance increments due to the increase in current density, Table 2 gives a comparison of the cell performance at different operating voltages under the optimization strategy. The values in the second column represented the current density when the assembly pressure was 0 and the GDL thickness was equal to 0.38 mm. The third column indicates the current density of the optimized model at different operating voltages. The fourth column shows the overall performance increment of the model after optimization. It can be seen that larger values of performance increment were observed at lower operating voltages. By optimizing the assembly pressure and GDL thickness, the cell current density was enhanced by 9.24% and 8.84% at 0.5V and 0.4V respectively compared to the base case.

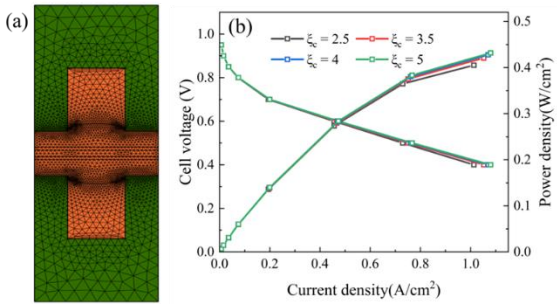

Fig. 5 (a) Reconstructed model of HT-PEMFC with assembly pressure of 1.38 MPa and GDL thickness of 0.375 mm. (b) Polarization curves and power density profiles of optimized HT-PEMFC at cathode stoichiometry ratios of 2.5, 3.5, 4 and 5, respectively.

Table 2. Current density increment at different voltages with optimized assembly pressure and GDL thickness.

Voltage (V)	Data in validation (A/cm^2)	Optimization parameters (A/cm^2)	current density increment (%)
0.95	0.00682	0.0068511	0.45
0.9	0.01596	0.016102	0.89
0.85	0.03539	0.036053	1.87
0.8	0.07189	0.074281	3.32
0.7	0.18057	0.19438	7.65
0.6	0.42041	0.45627	8.53
0.5	0.66813	0.72984	9.24
0.4	0.93061	1.0129	8.84

4.3 Combined effects of assembly pressure and GDL thickness on the variable distributions

Fig. 6a and 6b represent the impact on hydrogen distribution after optimizing the assembly pressure and GDL thickness. It was observed that the optimized fuel cell exhibited a greater discrepancy in hydrogen concentration. Employing an appropriate assembly pressure and GDL thickness could enhance the mass transfer of the anode assembly and optimize hydrogen utilization. Fig. 7a and 7b illustrate the impact of oxygen distribution after optimizing the assembly pressure and GDL thickness. The molar fraction of oxygen was greater in the gas channel than that below the ribs, with the maximum value observed in the gas channel and the minimum value beneath the ribs. Post-compression, the contrast in molar fraction between the rib region and gas channel became more pronounced, which was consistent with that reported by Sun et al.[15].

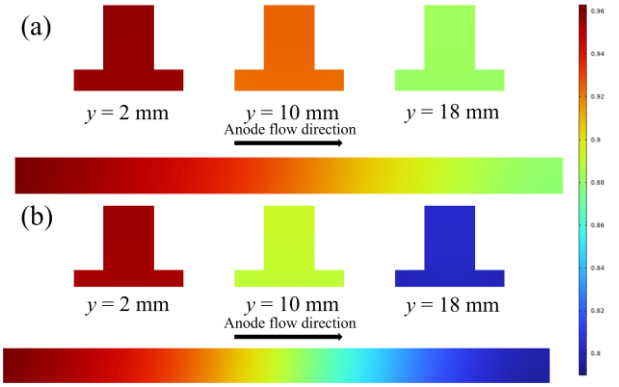

Fig.6. Hydrogen mole fraction distribution for unoptimized (a) and optimized (b) models in the y-z plane (x =1 mm) and x-z plane (y =2, 10, and 18 mm). The cell voltage is 0.4 V.

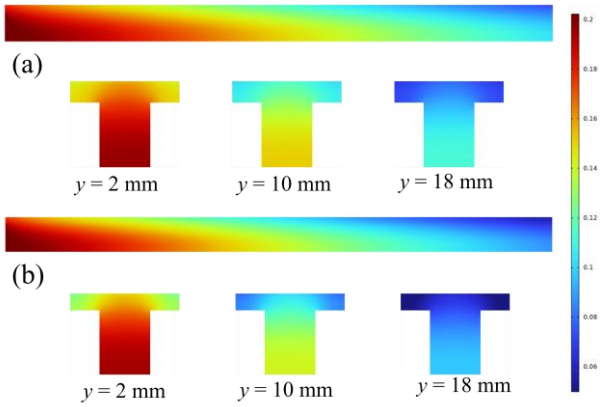

Fig.7. Oxygen mole fraction distribution for unoptimized (a) and optimized (b) models in the y-z plane (x =1 mm) and x-z plane (y =2, 10, and 18 mm). The cell voltage is 0.4 V.

The effect of optimized parameters on the temperature distribution of the fuel cell is shown in Fig. 8. Along the flow direction in the y-z plane, the temperature decreased, primarily influenced by the distribution of oxygen in that direction. In the x-z plane, the temperature was higher below the gas channel region, which was mainly because the heat was generated from the electrochemical reaction in the CL, and the gas channels were filled solely with gases of low thermal conductivity.

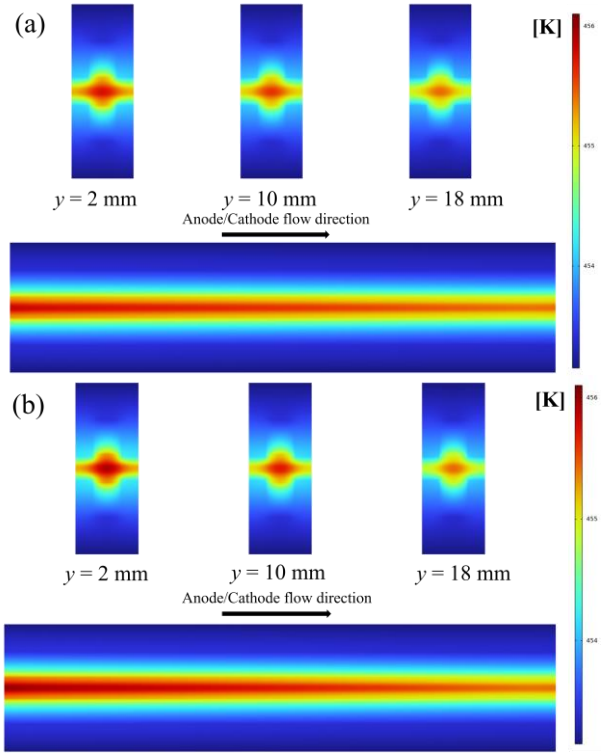

Fig. 8. Temperature distribution for unoptimized (a) and optimized (b) models in the y-z plane (x =1 mm) and x-z plane (y =2, 10, and 18 mm). The cell voltage is 0.4 V.

5. CONCLUSIONS

In this work, we developed a three-dimensional non-isothermal sequential model to investigate the combined impact of assembly pressure and GDL thickness on the performance of HT-PEMFC. RSM was utilized to comprehensively optimize these two parameters within the practical ranges of assembly pressure (0-2.5 MPa) and GDL thickness (0.1-0.5 mm). Through verification, it was found that the HT-PEMFC achieved its optimal overall performance at an assembly pressure of 1.38 MPa and GDL thickness of 0.375 mm, resulting in an improvement of approximately 9.24% compared to the initial case.

The research findings indicated that the compression of GDL caused by assembly pressure led to the non-uniform spatial distribution of porosity and permeability, as well as changes in the resistance at the GDL/BP interface. On the other hand, variations in GDL thickness affected the ohmic resistance and mass transfer resistance. Therefore, the changes in HT-PEMFC performance were the combined result of these two parameters. Additionally, the polarization curve, hydrogen distribution, oxygen distribution, and temperature distribution of HT-PEMFC were studied before and after optimization.

ACKNOWLEDGEMENT

This study was financially supported by the China Natural Science Foundation (Contract Nos. 21476073, 21176069, and 21878078).

REFERENCE

[1] R.K.A. Rasheed, Q. Liao, C. Zhang, S.H. Chan, A review on modelling of high temperature proton exchange membrane fuel cells (HT-PEMFCs), Int. J. Hydrogen Energy, 42 (2017) 3142-3165.

[2] R. Haider, Y. Wen, Z.F. Ma, D.P. Wilkinson, L. Zhang, X. Yuan, S. Song, J. Zhang, High temperature proton exchange membrane fuel cells: progress in advanced materials and key technologies, Chem. Soc. Rev., 50 (2021) 1138-1187.

[3] A. Diedrichs, M. Rastedt, F.J. Pinar, P. Wagner, Effect of compression on the performance of a HT-PEM fuel cell, J. Appl. Electrochem., 43 (2013) 1079-1099.

[4] A. Diedrichs, P. Wagner, Performance Analysis of a High-Temperature Polymer Electrolyte Membrane Fuel Cell under Mechanical Compression Control, ECS Trans., 50 (2012) 1137-1153.

[5] F.J. Pinar, M. Rastedt, N. Pilinski, P. Wagner, Effect of Compression Cycling on Polybenzimidazole-based High-Temperature Polymer Electrolyte Membrane Fuel Cells, Fuel Cells, 15 (2015) 140-149.

[6] T.J. Jaber, R. Jaralla, M. Sulaiman, K. Bourouni, Numerical Study on High Temperature PEM Fuel Cell (HTPEMFC), in, ICTEA: International Conference on Thermal Engineering: Theory & Applications, 2017.

[7] A. El-kharouf, T.J. Mason, D.J.L. Brett, B.G. Pollet, Ex-situ characterisation of gas diffusion layers for proton exchange membrane fuel cells, J. Power Sources, 218 (2012) 393-404.

[8] Y. Wang, D.F.R. Diaz, K.S. Chen, Z. Wang, X.C. Adroher, Materials, technological status, and fundamentals of PEM fuel cells - A review, Mater. Today, 32 (2020) 178-203.

[9] L. Xia, M. Ni, Q. He, Q. Xu, C. Cheng, Optimization of gas diffusion layer in high temperature PEMFC with the focuses on thickness and porosity, Appl. Energy, 300 (2021) 117357.

[10] T. Zhang, J. Li, Q. Li, M. Yu, H. Sun, Combination effects of flow field structure and assembly force on performance of high temperature proton exchange membrane fuel cells, Int. J. Energy Res., 45 (2021) 7903-7917.

[11] J. Ge, A. Higier, H. Liu, Effect of gas diffusion layer compression on PEM fuel cell performance, J. Power Sources, 159 (2006) 922-927.

[12] H. Kanani, M. Shams, M. Hasheminasab, A. Bozorgnezhad, Model development and optimization of operating conditions to maximize PEMFC performance by response surface methodology, Energy Convers. Manage., 93 (2015) 9-22.

[13] W.Z. Li, W.W. Yang, W.Y. Zhang, Z.G. Qu, Y.L. He, Three-dimensional modeling of a PEMFC with serpentine flow field incorporating the impacts of electrode inhomogeneous compression deformation, Int. J. Hydrogen Energy, 44 (2019) 22194-22209.

[14] H. Yuan, Y. Dai, H. Li, Y. Wang, Modeling of high-temperature polymer electrolyte membrane fuel cell for reaction spatial variation, Int. J. Heat Mass Transfer, 195 (2022) 123209.

[15] M. Sun, J. Huang, Z. Xia, S. Wang, G. Sun, Investigation of phosphoric acid and water transport in the high temperature proton exchange membrane fuel cells using a multiphase model, AIChE J., 68 (2022) e17708.